Engineering the Friction-and-Wear Behavior of Polyelectrolyte Multilayer Nanoassemblies Through Block Copolymer Surface Capping, Metallic Nanoparticles, and Multiwall Carbon Nanotubes

Prem V. Pavoor,[1] Brian P. Gearing,[2,*] Russell E. Gorga,[1] Anuj Bellare,[3] Robert E. Cohen[1]

[1]*Department of Chemical Engineering, Massachusetts Institute of Technology, Cambridge, Massachusetts 02139*
[2]*Department of Mechanical Engineering, Massachusetts Institute of Technology, Cambridge, Massachusetts 02139*
[3]*Department of Orthopaedic Surgery, Harvard Medical School, Brigham and Women's Hospital, Boston, Massachusetts 02115*

Received 1 August 2003; accepted 17 October 2003

ABSTRACT: In previous work, it was demonstrated that coating a surface with polyelectrolyte multilayers (PEMs) composed of polyallylamine hydrochloride (PAH) and poly(acrylic acid) (PAA) resulted in increased friction forces at low normal loads. At stress levels sufficient to cause system wear, however, PAH/PAA PEMs provided significant wear protection for the underlying substrate. This report evaluates three strategies for reducing the coefficients of friction associated with PEMs at low normal stress, while retaining their wear-retarding properties at high normal loads. Anchoring polystyrene-*block*-poly(acrylic acid) to the PAH surface of a multilayer film, less than 10 nm thick, enhanced the hardness, and hence the load-bearing capacity of these structures. The effect of surface capping was most pronounced at high normal stresses, where substantial wear prevention was observed, accompanied by low friction forces. These films are well suited for systems where wear particle generation hinders smooth operation. The second strategy used the *in situ* synthesis of silver nanoparticles in the PEM matrix for friction reduction. Optimum levels of silver clusters are required at the surface to reduce the friction forces. Finally, multilayer composites were constructed using PAH and multiwall carbon nanotubes. These assemblies exhibited the lowest values of friction among the strategies studied, at all levels of stress; in addition, substrate wear prevention was also achieved. The tribological behavior of the PEM-modification strategies was correlated with the mechanical properties of the films, elicited by nanoindentation. J Appl Polym Sci 92: 439–448, 2004

Key words: polyelectrolytes; tribology; block copolymers; nanocomposites; nanoindentation

INTRODUCTION

Surface modification, by soft organic coatings, has been employed extensively in the effort to alleviate the tribological problems associated with micromechanical device operation. Stiction, high friction forces, and wear remain the dominant issues,[1] particularly in those microelectromechanical systems (MEMS) with moving components subject to intermittent or continuous contact. Examples include motors, turbines, gear trains, actuators, valves, accelerometers, and display-device mirror assemblies.[2] Langmuir monolayers,[3] self-assembled thiol-based,[2] silane-based,[4–6] and alkene-based[7] monolayer films, and polymer films with layered architectures[8–11] have been investigated in this regard. The coatings demonstrate low friction forces; only some provide wear reduction of underlying substrates at higher normal stresses.[9–11]

These films require, however, either an intricate protocol for assembly[3] or a functionalized surface to which they can bind covalently.[2,4–11] The substrate, which in most cases is silicon, thus requires some level of pretreatment to present the desired functional groups. Generally, the pretreatment leads to the formation of a thin layer of oxide on the surface; charge trapping by this insulating layer can potentially lead to device failure.[5] Chlorosilane-based monolayers are also associated with release of corrosive byproducts, and the precursor molecules have the potential for bulk polymerization, which leads to particulate formation. Additionally, reproducibility and scale-up of the fabrication procedures for these surface modification techniques have proved challenging.[5]

Recently, the tribological properties of polyelectrolyte multilayers (PEMs), formed by the layer-by-layer adsorption of oppositely charged polyelectrolytes, have been studied.[12] Weak polyelectrolytes, poly-

**Present address:* School of Law (Boalt Hall), University of California, Berkeley, CA 94720-7200.

Correspondence to: R. Cohen (recohen@mit.edu).

Contract grant sponsor: Raymond A. and Helen E. St. Laurent Professorship in Chemical Engineering, MIT.

Contract grant sponsor: National Science Foundation; contract grant number: DMR 98-08921.

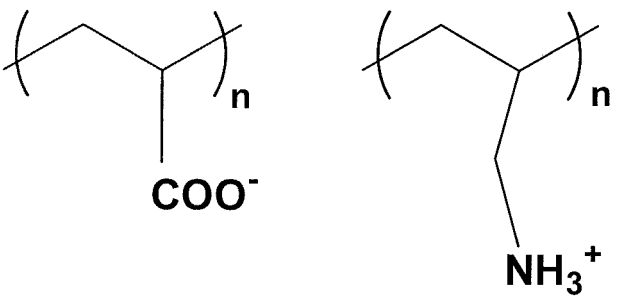

Figure 1 Structures of repeat units of PAA and PAH.

(acrylic acid) (PAA) and poly(allylamine hydrochloride) (PAH), were used in the investigation. The structures of the repeat units of the polyelectrolytes are depicted in Figure 1. The PEM assembly provides films that are easy to fabricate; assembly is automated[13] and proceeds at ambient conditions from aqueous solutions. The process is not associated with release of byproducts. Unlike other surface engineering techniques, PEMs can be assembled on a wide variety of substrates with little or no pretreatment. Strongly adhering PAH/PAA films, resistant to scotch-tape peel tests,[14] have been formed on metallic, plastic, glass, and silicon-based materials. Devices with complex architectures can be coated uniformly over large areas. PEMs are thus ideally suited to combat the tribological challenges in MEMS operations.

At low normal stresses, friction coefficients of PAH/PAA PEM-coated surfaces were higher than those exhibited by their uncoated counterparts.[12] These films, however, demonstrated a significant capacity for wear prevention of underlying stainless steel, glass, and silicon substrates at normal stresses up to 450 MPa and 2000 cycles of reciprocating motion. Delaminated film fragments prevented contact between the mating surfaces, avoiding wear. When assembled on the larger of the two contacting surfaces, a certain minimum film thickness ($\sim$ 20–30 nm for silicon substrates), depending on the substrate roughness, was required for consistent wear reduction without a substantial increase in the friction force. At higher thicknesses (above about 70 nm for silicon), PEMs provided reliable wear reduction; however, for the thicker films, adhesion to the counterface, deformation, and dragging of the fragments increased the friction forces over those observed for thinner films and the bare substrate (in the absence of its wear).[12]

The objective of this article is to discuss and evaluate strategies for engineering the PEM structure to reduce the friction coefficient (at lower normal stresses) without compromising its wear-preventing ability (at higher loads). The friction coefficient of the film (or its fragments) can be varied by altering its hardness, shear strength, or its adhesion to the counterface. In one strategy, we addressed these issues through surface capping of the PEM structure. Amphiphilic block copolymers were used to modify the surface properties of PEMs. By using one block to bind to the PEM surface, the other block can be chosen to decrease the adhesive component of friction of the PAH/PAA PEM surface, increase its hardness, or lower its resistance to orientation in the sliding direction. We selected polystyrene-*block*-poly(acrylic acid) (PS–PAA) to modify the surface of the PEM, noting that Choi and Rubner[15] successfully adsorbed PS–PAA onto PAH/PAA PEM surfaces. The PAA block was used for anchoring to the multilayer, thus exposing the PS block to the surface. Water contact angles as high as 85° after the treatment were reported[15] for films where the contact angle, before modification, was approximately 45°.

For a second strategy, we note that polymer composites with nanometer-sized metallic and ceramic filler particles were investigated for their tribological properties (see Yu et al.,[16] Sawyer et al.,[17] Voort and Bahadur,[18] Wang et al.,[19] and Petrovicova et al.[20]). The composites exhibit increased wear resistance compared with that of the unfilled polymer. Mixed results, however, have been reported about the effects of nanofillers on friction forces. PAH/PAA PEMs can serve as nanoreactors for the *in situ* synthesis of metallic and semiconducting particles.[21] At certain assembly pH values, the unused carboxylic acid functional groups in PAA can be used to bind various inorganic ions, which are then converted into nanoparticles by reduction or substitution chemistry. The process of incorporating nanoclusters in PAH/PAA PEMs can be repeated multiple times, systematically increasing both the mean particle size and volume fraction in the polymer matrix.[22] This technique offers a unique method of creating polymer nanocomposite coatings, with a variety of filler particles, that may demonstrate interesting friction and wear properties. We have chosen to study the effect of silver nanoclusters incorporated in PAH/PAA PEMs.

Finally, this article also discusses the friction-and-wear behavior of PEM structures that contain multiwall carbon nanotubes (MWNTs). Cumings and Zettl[23] demonstrated the reversible extension of a MWNT and suggested that these novel materials might serve as low-friction nanoscale linear bearings. Kotov and coworkers[24] constructed multilayer assemblies of negatively charged single-wall nanotubes and a cationic polyelectrolyte; tensile tests revealed enhanced mechanical properties for these structures. There is no reported literature on the friction and wear behavior of PEMs containing MWNTs.

In addition to tribological characterization of the modified PEM structures, nanoindentation was used

TABLE I
Average Coefficients of Friction μ for Surface-Capped PAH/PAA PEMs and PAH/MWNT Multilayer Composites, Assembled on Glass Substrates[a]

No.	Type of film	Film thickness (nm)	Average μ
1	Glass substrate	—	0.44 ± 0.24
2	(PAH 7.5/PAA 3.5)	5.5	0.45 ± 0.07
3	(PAH 7.5/PAA 3.5)	72	0.67 ± 0.04
4	(PAH 7.5/PAA 3.5) + PS–PAA	9.5	0.39 ± 0.01
5	(PAH 7.5/PAA 3.5) + PS–PAA	75	0.75 ± 0.16
6	$[(\text{PAH 2.5/PAA 2.5})_1(\text{PAH 2.5/MWNT 2.5})_5]_2$	140	0.21 ± 0.01
7	$[(\text{PAH 2.5/PAA 2.5})_1(\text{PAH 2.5/MWNT 2.5})_5]_6$	940	0.33 ± 0.05
8	$[(\text{PAH 2.5/PAA 2.5})_1(\text{PAH 2.5/MWNT 2.5})_5]_6$ Heated at 150°C, 6 h	940	0.26 ± 0.04

[a] Normal stress: 250 kPa.

to correlate the friction-and-wear behavior of the films with their mechanical properties.

EXPERIMENTAL

PAH (M_w = 70,000), silver acetate, octadecyltrichlorosilane (OTS), toluene, and tetrahydrofuran (THF) were purchased from Sigma–Aldrich (Milwaukee, WI). PAA (M_w = 90,000) was obtained from Polysciences (Warrington, PA). PS–PAA (M_n of PS block = 16,500, M_n of PAA block = 4500, M_w/M_n = 1.05) was purchased from Polymer Source Inc. (Dorval, Canada). MWNTs, 1–5 μm in length and 20–50 nm in diameter, were obtained from NanoLab (Brighton, MA). Nitric acid (70%) and hydrogen peroxide (30%) were purchased from EM Science (Gibbstown, NJ). Sulfuric acid was obtained from Mallinckrodt Baker, Inc. (Paris, KY), and BOC Gases (Murray Hill, NJ) supplied hydrogen (grade 4.7) and nitrogen (grade 5). All these materials were used without further purification. Deionized water (>18 MΩ cm^{-1}, Millipore Milli-Q, Milford, MA) was used for preparation of all aqueous solutions, and during rinsing procedures.

Stainless-steel sheets (type 316, #8 mirror finish), with an average roughness of approximately 6 nm, were purchased from McMaster-Carr (Dayton, NJ). Polished single-crystal silicon wafers of ⟨100⟩ orientation were obtained from Nestec, Inc. (New Bedford, MA). Glass microscope slides from VWR Scientific Inc. (West Chester, PA) were used. The average roughness for the glass and silicon substrates did not exceed 1 nm. These materials were all used as substrates for PEM assembly.

PAH/PAA PEMs were assembled on these substrates as previously described.[12,13] The films were assembled at a pH of 7.5 or 3.5 for the PAH solution, and a pH of 3.5 for PAA, referred to as PAH 7.5/PAA 3.5 or PAH 3.5/PAA 3.5. The films were flushed with air at room temperature and stored at ambient conditions for several hours before further processing.

PAH 7.5/PAA 3.5 films, constructed with PAH as the last adsorbed layer, were immersed in PS–PAA solution in THF (0.001*M* based on the molecular weight of the PAA repeat unit, pH unadjusted) for 15 min, following reported protocol.[15] They were then rinsed twice in pure THF for 1 min, before drying in air.

PAH 3.5/PAA 3.5 films, with PAA adsorbed last, were used as matrices for silver nanocluster synthesis. The experimental procedure was described in detail in Joly et al.[21] and Wang et al.[22] Films, originally 70 nm thick, with 1, 3, and 5 silver ion load and reduction cycles were prepared following the literature procedure.

PAH/MWNT multilayer composites were constructed using a protocol adapted from Mamedov et al.[24] A suspension of MWNTs was refluxed in 70% nitric acid for 6 h. The acid was subsequently removed using centrifugation, and replaced with deionized water. The treatment with nitric acid leads to partial oxidation of the carbon nanotubes.[25] Sonication of the suspension resulted in a stable aqueous dispersion of the MWNTs. For multilayer assembly, a PAH 2.5/PAA 2.5 bilayer was first deposited on the substrate to promote film adhesion. This was followed by five layers of PAH 2.5/MWNT 2.5. After every fifth layer of PAH/MWNT, a PAH/PAA bilayer was deposited to promote stable film growth, as recommended by Kotov and coworkers.[24] The resulting structure is represented as $[(\text{PAH 2.5/PAA 2.5})_1/(\text{PAH 2.5/MWNT 2.5})_5]_x$, where x (see Table I) denotes the number of times the cycle was repeated. Dipping times of 15 min for PAH and PAA, and 60 min for the MWNT dispersion were used. After exposure to each solution, the substrate was subject to three rinsing steps in water for 2, 1, and 1 min, respectively. The MWNTs were the last adsorbed material in all cases.

Self-assembled monolayer films of OTS were assembled on silicon substrates to compare their performance with PEMs. Silicon slides were treated with

piranha solution (3 : 1 volume ratio of sulfuric acid and 30% hydrogen peroxide) for 30 min at 90°C. After washing with water and ethanol, the substrate was dried in a stream of nitrogen. Subsequently, it was immersed in a solution of OTS in toluene (0.001*M*) for 60 min. The resulting monolayer was rinsed with acetone and ethanol, and dried by flushing with nitrogen.

Thicknesses of PEM films on glass substrates were measured using a Tencor P-10 surface profiler. For films less than 10 nm thick, a Gaertner L116 ellipsometer was used to measure thickness; silicon was used as the substrate. Contact angle measurements were carried out using a goniometer (Ramé–Hart, Mountain Lakes, NJ). In all cases, average values were obtained after measurements at three to five locations at ambient conditions.

For transmission electron microscopy (TEM) of MWNT multilayer composites, films were deposited on silicon nitride grids obtained from Structure Probe, Inc. (West Chester, PA); details about the grid structure are given in Boontongkong and Cohen.[26] Imaging was performed on a JEOL 200CX (JEOL, Peabody, MA) operated at 200 kV.

Friction-and-wear behavior was studied using a flexure-based biaxial apparatus as described in Gearing and Anand.[27] Flat-on-flat configurations were used for all tests. The upper cylindrical pin with a flat surface, 1 or 2 mm in diameter, was held stationary and the lower, larger surface was subject to reciprocating motion over a 3-mm path length. In all the experiments, uncoated and film-coated substrates were mounted on the lower slider using double-coated paper scotch tape. The 1-mm-diameter pin, used for wear studies at large normal stresses, was made of D2 hardened tool steel, whereas the 2-mm-diameter counterface, for friction tests at 250 kPa, was made of type 316 stainless steel. Between tests, these pins were polished against 1-μm aluminum oxide film-coated disks using a specially designed pin holder to maintain a flat surface. The polished pins were subsequently cleaned with acetone and dried in a blast of air. A sliding speed of 200 μm/s was used in all tests. The number of cycles was confined to 20–30, corresponding to an accumulated sliding distance between 120 and 180 mm. The humidity in the test area was not controlled; it varied in the 15–55% range over the duration of the test period.

Wear tracks, obtained during the tribological tests, were examined using an optical microscope. Wear was also characterized by examining the cross section of the wear track with a profilometer. The wear track was examined at three different points; in all cases, the surface profiles closely resembled each other.

Mechanical behavior of PEMs, assembled on glass substrates, was characterized using a nanoindenter (TriboIndenter, Hysitron, Inc., Minneapolis, MN); a diamond Berkovich tip, with a tip radius between 100 and 200 nm, was used in most cases. Maximum loads between 75 and 1000 μN were applied using a trapezoidal load function consisting of a 5-s loading segment, 2-s hold time, and 5-s unloading segment. For the 6000-nm-thick PAH 7.5/PAA 3.5 film, the load and unload segments were of a 33-s duration. Penetration depths varied between 50 and 300 nm for films 1000–6000 nm in thickness. To achieve penetration depths less than 10 nm, a NorthStar 90° cube-corner diamond indenter tip was used; the tip radius was approximately 40–50 nm. A maximum load of 4 μN was applied using the 5-s/2-s/5-s load function described earlier. In all cases, the unloading segments of the indentation curves were used to elicit values of film hardness and effective modulus (E_r), as suggested by Oliver and Pharr.[28] Both the indenter tip and indented materials contribute to E_r, given by the following equation:

$$\frac{1}{E_r} = \frac{(1 - \nu_s^2)}{E_s} + \frac{(1 - \nu_i^2)}{E_i} \quad (1)$$

The subscripts s and i refer to the sample and the indenter; E and ν denote the elastic modulus and Poisson's ratio. For the cube-corner indenter, the relation between the contact area and the distance from the indenter tip was accurately calibrated using a fused quartz sample of known mechanical properties. An approximate relation, based on ideal tip geometry,[28] was used for the Berkovich tip. The temperature was maintained in the 20–25°C range; the ambient humidity was approximately 50%.

RESULTS AND DISCUSSION

Two levels of normal stress were investigated to elucidate the tribological merit of the PEM modification strategies. Films assembled on glass substrates were tested at a low normal stress of 250 kPa, based on the diameter of the pin, to elicit their frictional response without a dominating influence of substrate wear on the results. Table I depicts the average values of the steady-state friction coefficients μ exhibited by film-coated glass slides over 20 cycles of reciprocating motion, for the unmodified PEMs and for the surface capping and MWNT composite strategies.

Choi and Rubner[15] recommend the PAH 7.5/PAA 3.5 system, with PAH adsorbed last, for enhanced adsorption of the PS–PAA block copolymer. At this pH combination, the surface of the PEM structure is enriched with functional groups from the last adsorbed polyelectrolyte.[29] The amine groups of PAH offer anchoring sites for the acid-containing PAA blocks of the copolymer. The advancing contact angle with water increased from 42° for the PAH/PAA film

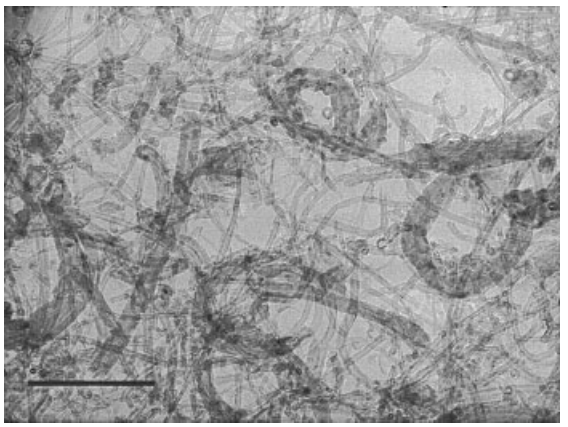

Figure 2 Plan-view TEM image of a [(PAH 2.5/PAA 2.5)$_1$(PAH 2.5/MWNT 2.5)$_5$] 140-nm-thick multilayer composite. Scale bar depicts 500 nm.

to 86° after adsorption of PS–PAA, in agreement with previously reported work.[15] Two thicknesses for surface-capped PEMs were studied: 9 nm and approximately 70 nm. Friction coefficients μ for the PAH/PAA PEM, before surface modification, are also reported in Table I. For both thicknesses, the friction forces were only slightly affected after the capping (compare lines 2 and 4 and lines 3 and 5 of Table I).

Figure 2 depicts a plan-view TEM image of a 140-nm-thick multilayer composite containing MWNTs. The MWNTs are well dispersed in the multilayer; only a few large aggregates were seen. Table I (lines 6 and 7) reports friction coefficients for this film and for its 940-nm-thick counterpart. The latter film was also thermally crosslinked by heating at 150°C for 6 h[30]; line 8 shows its associated μ value. The 140-nm PAH/MWNT film exhibited the lowest friction force, with a coefficient only slightly above 0.2.

PAH 3.5/PAA 3.5 films, 70 nm in thickness, were chosen as the matrix for the *in situ* introduction of silver nanoclusters. This assembly pH combination is associated with unionized carboxylic acid groups that may be used for silver ion loading[22]; subsequent reduction using hydrogen gas results in 3- to 4-nm-diameter silver nanoparticles. This process may be repeated to increase the size and volume fraction of the silver clusters. Figure 3 depicts friction coefficients for PEMs after one, three, and five cycles of silver loading and reduction; the friction coefficient for the unfilled 70-nm-thick PEM is also depicted. The film with three load-and-reduction cycles exhibited the lowest average coefficient of friction of 0.3 in this series of specimens.

The wear behavior of surface-capped PAH/PAA PEMs is presented in Figure 4. Silicon substrates were used for these tests, carried out at a normal stress of 4 MPa. Figure 4 depicts the maximum and minimum steady-state friction coefficients observed over two to three tests for each configuration, over 20 cycles of reciprocating motion. For the case of bare silicon, mixed results were observed. In the absence of system wear, the friction was confined to a low value of 0.12; wear particles increased the value to as high as 0.7. A self-assembled monolayer of OTS, currently the preferred surface modification technique in MEMS devices,[1] was tested for comparison; this 1.5- to 2-nm film exhibited an advancing water contact angle of 101°. In the best case, the film lowered the friction coefficient to 0.07 without system wear. For two of the three experiments, however, system wear occurred within the first few cycles, leading to high friction coefficients. By comparison, a 6-nm PAH/PAA PEM was unable to prevent system wear, resulting in friction coefficients in the 0.4–0.7 range. When the same film was surface capped with the block copolymer, no wear was observed in all three experiments. The friction coefficient was restricted to a narrow window between 0.22 and 0.26. Films that were 70 nm thick prevented system wear in both the native and capped forms; the associated friction coefficients were comparable.

Wear tests on stainless steel substrates were conducted at a normal stress of 1 MPa. PEMs (70 nm thick), unfilled and containing one loading cycle of silver nanoparticles, and a 200- to 250-nm PAH/MWNT composite were tested. The average friction coefficients and wear results are presented in Table II. Except for the bare substrate, wear prevention of the steel slider was observed in all cases. Figure 5 shows optical micrographs and cross-sectional surface profiles of the wear tracks, for the case of the bare substrate, and the unfilled and silver-containing PEM-coated slider; in the latter two cases, the wear of the steel substrate was significantly reduced. The optical micrograph and cross-sectional profile for the MWNT multilayer composite-coated steel surface, after the test, are depicted in Figure 6.

Results from nanoindentation studies on the modified PEM structures are presented in Table III. Because the indenter tip was diamond, E_i = 1140 GPa, and ν_i =

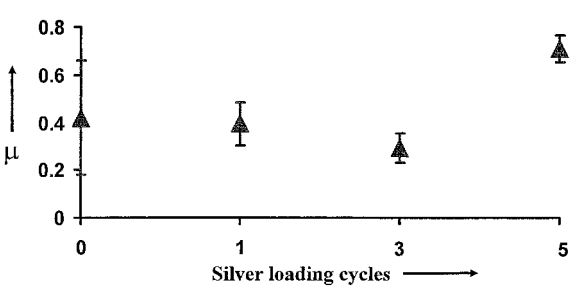

Figure 3 Average friction coefficients for silver-containing PAH/PAA PEMs assembled on glass. In all cases, native film was assembled at the (PAH 3.5/PAA 3.5) combination and was approximately 70 nm thick. Normal stress: 250 kPa.

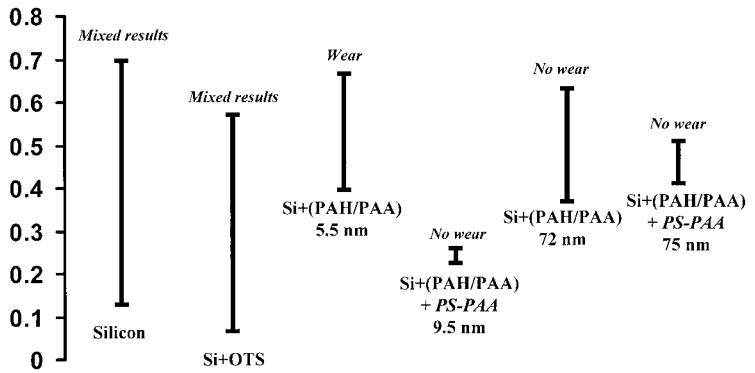

Figure 4 Maximum and minimum steady-state friction coefficients, and wear behavior of native and PS–PAA surface-capped PAH/PAA PEMs on silicon substrates at a normal stress of 4 MPa.

0.07 [see eq. (1)]. For most materials $E_i \gg E_s$, and the contribution of the second term in the equation is negligible. The Poisson's ratio for a range of polymeric materials lies between 0.25 and 0.45; E_s is thus 80–95% of the value of E_r. Tip penetration was quantified by the contact depth, which corrects the penetration depth at peak load for the deflection of the surface at the contact perimeter.[28] Based on literature recommendations,[31] contact depths were limited to 10–15% of the film thickness to eliminate contributions from the glass substrate, associated with an elastic modulus of 70 GPa.[28] Detailed analysis, to be reported in a forthcoming publication, was carried out to confirm the validity of this recommendation. To establish that the choice of indenter geometry did not significantly affect results, 6000-nm-thick PAH 7.5/PAA 3.5 films were indented to approximately the same contact depths with the Berkovich and cube-corner indenter tip. Table III (lines 1 and 2) reveals only a 13% difference in the values of E_r.

The flat pin-on-slider geometry used here, and previously,[12] introduces a degree of plowing at both the kPa and MPa stress levels, causing delamination of the film. In the absence of substrate wear, adhesion of the PEM fragments to the counterface, their deformation, and dragging at the interface increase the friction forces above those exhibited by the bare substrate (Table I, lines 1 and 3). We hypothesized that tuning the hardness, adhesive friction component, or shear strength of the PEM fragments would alter the friction coefficients. Adsorption of the PS–PAA block copolymer lowers the hydrophilicity of the PAH/PAA PEM as reflected by an increase in the water contact angle. The 3- to 4-nm-thick PS block,[15] below its glass-transition temperature, is not expected to be amenable to orientation in the sliding direction and thereby alter the shear strength of the film. At a normal stress of 250 kPa, the friction force for a 9-nm capped film was only marginally lower than that of the uncapped film (Table I, lines 2 and 4). At higher stresses, however, the effect of the surface capping was more pronounced (see Fig. 4). The 9-nm-thick film prevented system wear repeatedly, accompanied by friction coefficients in the 0.20–0.25 range. The uncapped control did not demonstrate wear prevention capability. The improved friction-and-wear behavior can be explained, not by a decrease in the adhesion friction component attributed to the reduced hydrophilicity, but by improved mechanical behavior for the capped structure. At thicknesses less than 10 nm, the block copolymer contributes to 40–50% of the total film thickness, and hence significantly to the mechanical response. Indentation studies, using contact depths of 8–9 nm, revealed that the modulus and hardness of the capped structure were 60% higher than those of its uncapped counterpart (Table III, lines 3 and 4). This translates into a larger load-bearing capacity and a lower degree of asperity penetration for the capped film, during

TABLE II
Wear Behavior of Silver Nanoparticle- and MWNT-containing PEMs on Steel Substrates[a]

No.	Type of film	Thickness (nm)	Substrate wear?	Average μ
1	—	—	Yes	0.57
2	(PAH 3.5/PAA 3.5)	70	No	0.76
3	(PAH 3.5/PAA 3.5) + Silver (1 Loading)	70	No	0.60
4	$[(\text{PAH 2.5/PAA 2.5})_1(\text{PAH 2.5/MWNT 2.5})_5]_2$	200–250	No	0.27

[a] Normal stress: 1 MPa.

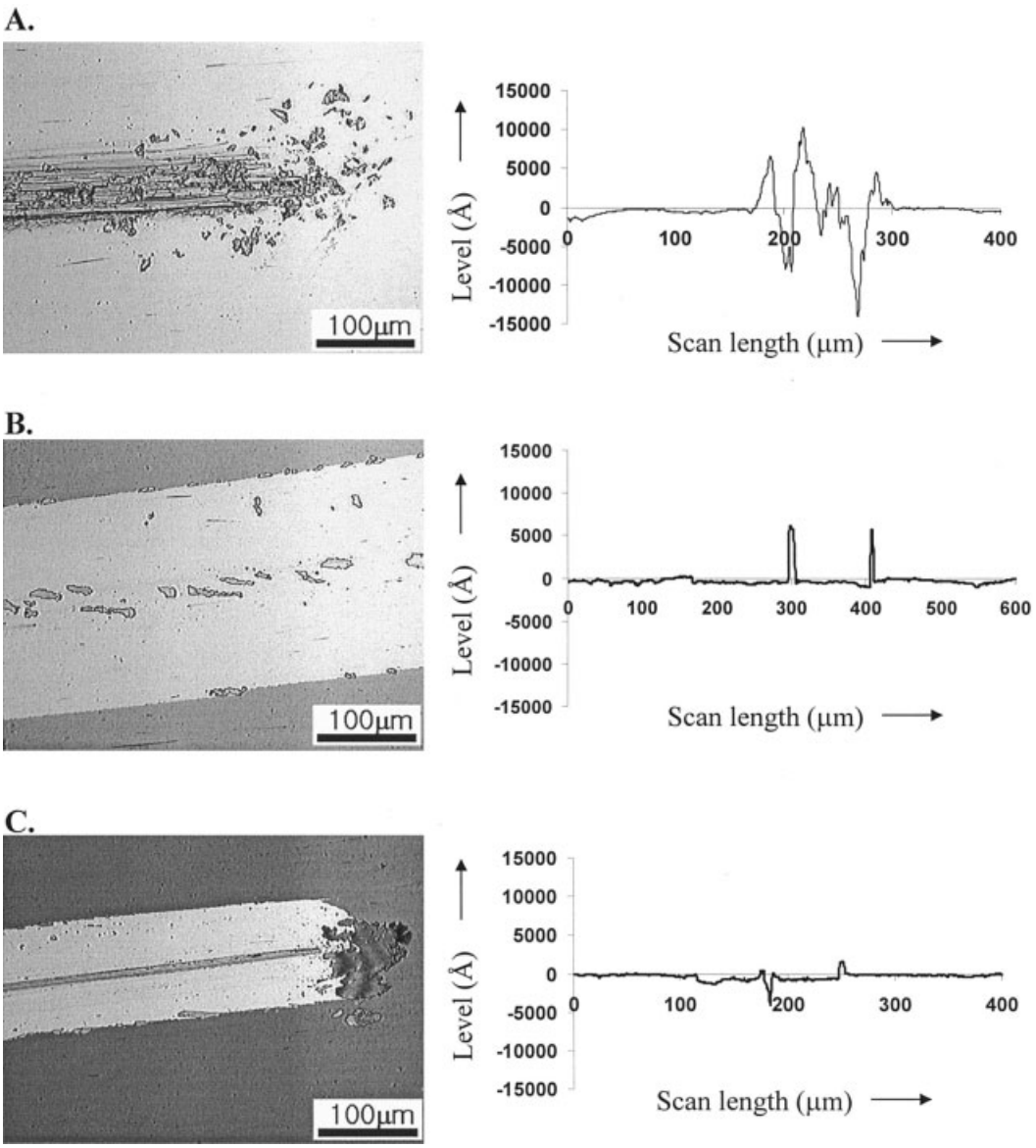

Figure 5 Optical micrographs and cross-sectional wear track profiles on (A) bare steel, (B) 70 nm (PAH 3.5/PAA 3.5) PEM-coated steel, and (C) 70-nm-thick PEM-coated steel containing one silver loading cycle. Test was carried out at 1 MPa normal stress and 30 cycles of reciprocating motion. In all cases, the steel substrate is at level zero.

sliding. The improved tribological performance was especially evident at higher stresses. By comparison, monolayers of OTS (Fig. 4) do not demonstrate wear prevention at these high loads.

At higher thicknesses (~ 70 nm) the block copolymer contributes to only about 5% of the film thickness. The underlying PEM matrix thus dominates the mechanical properties. Table III (lines 1 and 5) depicts the hardness and modulus values of the native and capped structure after indenting to contact depths much greater than the thickness of the block copolymer; essentially, no difference was observed between the capped and uncapped films. There is enough film material at the interface, in both cases, to prevent wear of the system at 4 MPa (see Fig. 4), and the friction coefficients (~ 0.6–0.7; see Table I, lines 3 and 5) depend mainly on the conformation of the fragments at the sliding interface.

At stresses causing system wear, approximately 10-nm-thick PS–PAA capped PAH/PAA PEMs demonstrate consistently low values of friction coupled with substrate wear prevention. With an increase in film thickness, however, the efficacy of the block copolymer–capped PEM with respect to friction reduction is lost.

Silver nanoclusters, introduced *in situ* into PAH/PAA PEMs, are expected to facilitate sliding, at lower normal stresses, by transferring contact off the polymer matrix. An optimum amount of silver is needed at the surface to reduce the friction coefficient reliably;

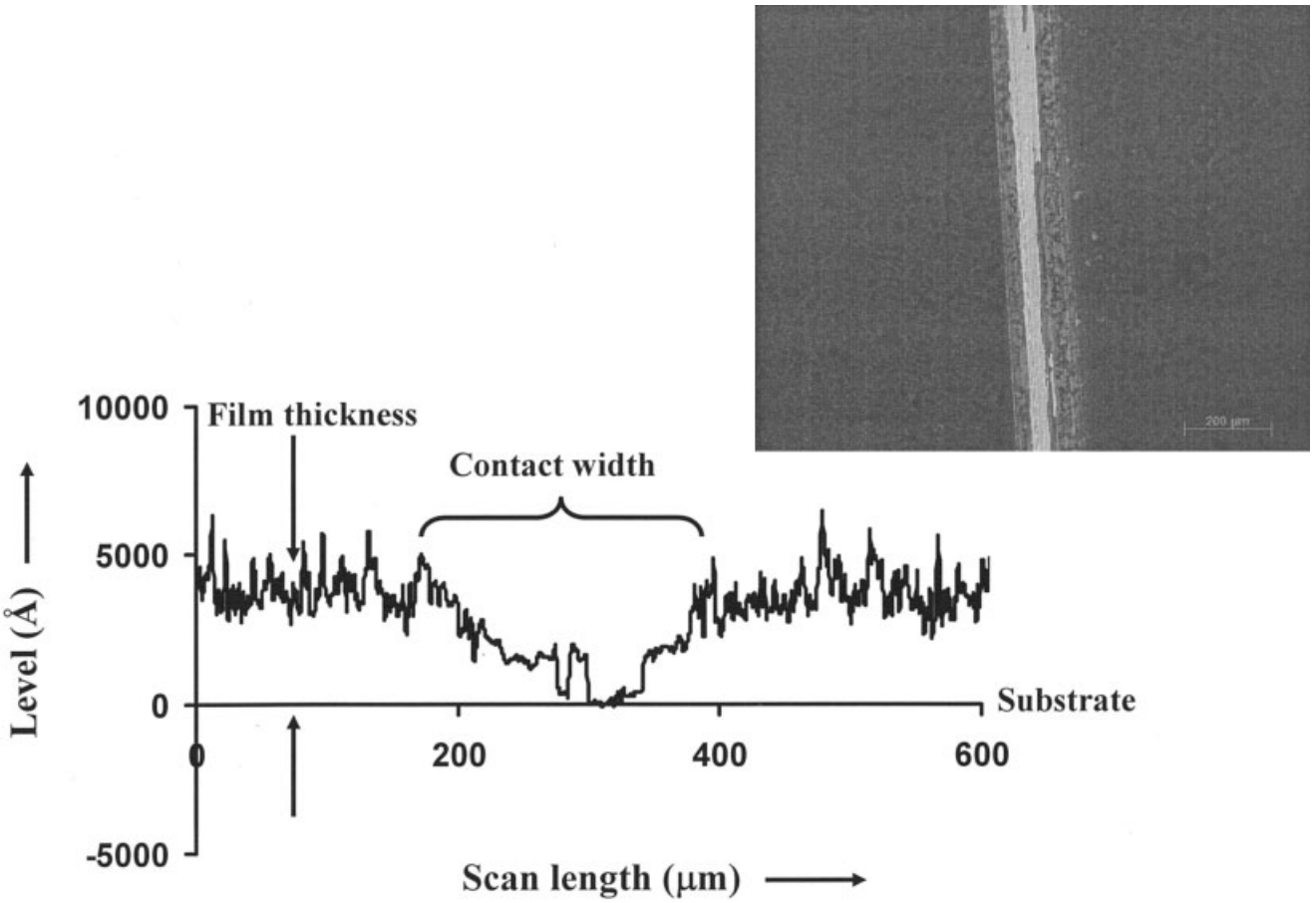

Figure 6 Optical micrograph and cross-sectional surface profile of wear track on PAH/MWNT composite-coated steel after 30 cycles of reciprocating motion at a normal stress of 1 MPa; substrate is at level zero.

an excess of silver can increase friction through a third-body effect. This trend is reflected in Figure 3. Three loading cycles of silver exhibited the lowest coefficient, whereas a substantial increase in friction was observed after five loading cycles. Nanoindentation studies on an unfilled and once-loaded, silver-containing PEM revealed comparable mechanical properties (see Table III, lines 6 and 7); mechanical reinforcement of the film structure attributed to the silver particles was not observed. The nanoparticles occupy 5.5% of the film, by volume, after one loading and reduction cycle.[22] After five loading cycles, the volume fraction increased to 17%. In the absence of a substantially high volume fraction of silver, the poly-

TABLE III
Mechanical Properties of PEM Assemblies Through Nanoindentation

No.	Type of film	Approximate film thickness (nm)	Indenter tip	Contact depth (nm)	Reduced modulus E_r (GPa)	Hardness (GPa)
1	(PAH 7.5/PAA 3.5)	6000	Berkovich	316 ± 10	12.6 ± 0.5	0.39 ± 0.03
2	(PAH 7.5/PAA 3.5)	6000	Cube-corner	312	10.9	0.36
3	(PAH 7.5/PAA 3.5)	100	Cube-corner	8.4 ± 1.0	7.9 ± 1.0	0.76 ± 0.09
4	(PAH 7.5/PAA 3.5) + PS–PAA	100	Cube-corner	8.9 ± 0.7	12.9 ± 2.4	1.23 ± 0.18
5	(PAH 7.5/PAA 3.5) + PS–PAA	6000	Berkovich	124 ± 9	10.8 ± 0.7	0.35 ± 0.06
6	(PAH 3.5/PAA 3.5)	1300	Berkovich	55 ± 10	19.2 ± 2.6	0.96 ± 0.26
7	(PAH 3.5/PAA 3.5) + Silver (1 loading)	1300	Berkovich	56 ± 3	20.2 ± 1.0	0.86 ± 0.15
8	$[(PAH\ 2.5/PAA\ 2.5)_1(PAH\ 2.5/MWNT\ 2.5)_5]_6$	940	Berkovich	196 ± 24	1.1 ± 0.3	0.04 ± 0.02
9	$[(PAH\ 2.5/PAA\ 2.5)_1(PAH\ 2.5/MWNT\ 2.5)_5]_6$ Heated at 150°C, 6 h	940	Berkovich	181 ± 35	1.5 ± 0.7	0.06 ± 0.04

mer matrix will determine wear behavior of the film at higher stresses. The friction coefficient for a once-loaded, silver-containing film at a normal stress of 1 MPa was slightly lower than the unfilled PEM (Table II, compare lines 2 and 3). The values of μ, however, are mainly governed by the conformation of the interface film fragments at these stresses. Optical micrographs and surface profiles (Fig. 5) depict significant prevention of substrate wear for PEM-coated systems, in accordance with previous work.[12]

Silver-containing PEMs offer the advantage of a wear-preventing PEM matrix at high normal loads, and a low friction surface (compared to the native film) at lower stresses. It is unclear whether the choice of nanoparticle will affect the friction coefficient. The general nanocluster incorporation scheme,[21] like the one presented by PAH/PAA PEMs, offers the possibility of introducing a wide variety of nanoparticles of metals and metallic compounds into the polymer matrix, and studying their effect on tribological behavior.

From Table III, it is clear that the assembled PAH/MWNT composites were significantly softer than their PAH/PAA counterparts. Nanoindentation studies, reported in a separate publication, revealed that the mechanical properties of the composites were comparable to those of thin films of PAH. The individual MWNTs, used as the anionic material, can be displaced easily during indentation, leading to modulus and hardness values that are close to those of the surrounding polyelectrolyte matrix.

Both Table I and II reflect the tribological merit of this easy-to-shear carbon nanotube-containing material. The friction coefficients are the lowest observed in this study, even for a 940-nm film. Thermally converting the ionic PAH–MWNT surface attachments to covalent amide bonds does not reinforce the PAH polymer matrix; the friction coefficient (Table I, lines 7 and 8) and hardness (Table III, compare lines 8 and 9) values are comparable. The nature of surface bonds may play a role in the presence of a liquid, where the films behave like hydrogels,[32] responsive to the pH and ionic strength of the surrounding medium. The PAH/MWNT composites also exhibit values of μ as low as 0.27 at higher stresses, as depicted in Table II; this is in addition to substrate wear prevention. From Figure 6 it is clear that a considerable portion of the film remains attached to the wear track. MWNT multilayer composites thus show merit for both friction and wear reduction. The multilayer assembly technique offers a facile way to create low friction surfaces by exploiting the properties of MWNTs.

CONCLUSIONS

This article has evaluated three strategies for tuning the friction forces exhibited by polyelectrolyte multilayers, while sustaining (or enhancing) their wear-retarding properties. PAH/PAA PEMs, less than 10 nm thick and capped with the PS–PAA block copolymer, exhibited enhanced substrate wear prevention at high stresses compared with the uncapped counterpart; this was in addition to maintaining low friction forces. These films are ideally suited for devices where wear particle generation leads to high friction forces and hinders smooth operation. The introduction of silver nanoparticles into PEMs had a beneficial tribological effect at low normal stresses; an optimum amount of surface silver is required for low friction coefficients. At higher stresses, the tribological behavior of these composites was dominated by the surrounding PEM matrix. The general scheme of nanoparticle synthesis offered by these films makes it possible to study the effect of various nanoparticle types on friction. Finally, novel PEM–MWNT composites, demonstrating low friction and wear at all levels of stress, were assembled. These multilayer composite coatings exhibited the lowest values of friction forces among the strategies studied. Nanoindentation was successfully used to correlate the mechanical properties of these structures with their observed tribological behavior.

In all cases, these polyelectrolyte multilayer films provided a wear-preventing coating associated with a well-defined friction force. PEM-based assemblies are ideally suited to combat the tribological challenges in a number of applications using different bearing materials.

This research was supported by the Raymond A. and Helen E. St. Laurent Professorship in Chemical Engineering, MIT, and by the MIT MRSEC program of the National Science Foundation under award number DMR 98-08941.

The research used the biaxial apparatus in the laboratory of Prof. Lallit Anand, MIT Department of Mechanical Engineering; the optical microscope in the laboratory of Prof. Paula Hammond, MIT Department of Chemical Engineering; and the goniometer and ellipsometer in the laboratory of Prof. Paul Laibinis, MIT Department of Chemical Engineering. In addition, experimental facilities at the MIT Center for Materials Science and Engineering and the MIT Nanomechanical Technology Laboratory were used. The authors acknowledge Alan Schwartzman, MIT Nanomechanical Technology Laboratory, for assistance with indentation studies. The authors also thank Dr. Dehua Yang, Hysitron, Inc., for the three data entries in Table III that used the cube-corner indenter tip. Manish Bajaj is thanked for help with preparing self-assembled monolayers, and with ellipsometric and contact angle measurements. The authors thank Jeeyoung Choi for helpful discussions on the block copolymer surface capping of PEMs. In addition, the authors thank Prof. Michael Rubner, MIT Department of Materials Science and Engineering; Prof. Lallit Anand and Prof. Mary Boyce, MIT Department of Mechanical Engineering; Dr. Tom Wang; and Dr. Yizhak Sabba for insightful discussions and help during the various stages of the study. The authors also acknowledge Yonathan Thio, Heejae Kim, and Nicoli

Ames for help during the project, and Peter Morley, MIT Machine Shop, for expertise in designing the mating surfaces for the biaxial apparatus.

References

1. Komvopoulos, K. Wear 1996, 200, 305.
2. Sundararajan, S.; Bhushan, B. In: NATO Advanced Study Institute on Fundamentals of Tribology and Bridging the Gap between the Macro- and Micro/Nano Scales; Bhushan, B., Ed.; Kluwer Academic: Keszthely, Hungary, 2000; pp. 821–850.
3. Tsukruk, V. V.; Bliznyuk, V. N.; Hazel, J.; Visser, D.; Everson, M. P. Langmuir 1996, 12, 4840.
4. DePalma, V.; Tillman, N. Langmuir 1989, 5, 868.
5. Maboudian, R.; Ashurst, W. R.; Carraro, C. Tribol Lett 2002, 12, 95.
6. Srinivasan, U.; Howe, R. T.; Maboudian, R. In: Tribology Issues and Opportunities in MEMS; Bhushan, B., Ed.; Kluwer Academic: Dordrecht, The Netherlands, 1998; pp. 597–605.
7. Ashurst, W. R.; Yau, C.; Carraro, C.; Lee, C.; Kluth, G. J.; Howe, R. T.; Maboudian, R. Sens Actuators A 2001, 91, 239.
8. Tsukruk, V. V.; Nguyen, T.; Lemieux, M.; Hazel, J.; Weber, W. H.; Shevchenko, V. V.; Klimenko, N.; Sheludko, E. In: Tribology Issues and Opportunities in MEMS; Bhushan, B., Ed.; Kluwer Academic: Dordrecht, The Netherlands, 1998; pp. 607–614.
9. Tsukruk, V. V. Tribol Lett 2001, 10, 127.
10. Julthingpiput, D.; Ahn, H.; Kim, D.; Tsukruk, V. V. Tribol Lett 2002, 13, 35.
11. Sidorenko, A.; Ahn, H.; Kim, D.; Yang, H.; Tsukruk, V. V. Wear 2002, 252, 946.
12. Pavoor, P. V.; Gearing, B. P.; Bellare, A.; Cohen, R. E. Wear, to appear.
13. Yoo, D.; Shiratori, S. S.; Rubner, M. F. Macromolecules 1998, 31, 4309.
14. Hidber, P. C.; Helbig, W.; Kim, E.; Whitesides, G. M. Langmuir 1996, 12, 1375.
15. Choi, J.; Rubner, M. F. J Macromol Sci Pure Appl Chem 2001, A38, 1191.
16. Yu, L.; Yang, S.; Wang, H.; Xue, Q. J Appl Polym Sci 2000, 77, 2404.
17. Sawyer, W. G.; Freudenberg, K. D.; Bhimaraj, P.; Schadler, L. S. Wear, to appear.
18. Voort, J. V.; Bahadur, S. Wear 1995, 181, 212.
19. Wang, Q.; Xue, Q.; Shen, W.; Zhang, J. J Appl Polym Sci 1998, 69, 135.
20. Petrovicova, E.; Knight, R.; Schadler, L. S.; Twardowski, T. E. J Appl Polym Sci 2000, 78, 2272.
21. Joly, S.; Kane, R.; Radzilowski, L.; Wang, T.; Wu, A.; Cohen, R. E.; Thomas, E. L.; Rubner, M. F. Langmuir 2000, 16, 1354.
22. Wang, T. C.; Rubner, M. F.; Cohen, R. E. Langmuir 2002, 18, 3370.
23. Cumings, J.; Zettl, A. Science 2000, 289, 602.
24. Mamedov, A. A.; Kotov, N. A.; Prato, M.; Guldi, D. M.; Wicksted, J. P.; Hirsch, A. Nat Mater 2002, 1, 190.
25. Mawhinney, D. B.; Naumenko, V.; Kuznetsova, A.; Yates, J. T.; Liu, J.; Smalley, R. E. Chem Phys Lett 2000, 324, 213.
26. Boontongkong, Y.; Cohen, R. E. Macromolecules 2002, 35, 3647.
27. Gearing, B. P.; Anand, L. In: Proceedings of the 2001 ASME International Mechanical Engineering Congress and Exposition, New York, New York, 2001.
28. Oliver, W. C.; Pharr, G. M. J Mater Res 1992, 7, 1564.
29. Shiratori, S. S.; Rubner, M. F. Macromolecules 2000, 33, 4213.
30. Harris, J. J.; DeRose, P. M.; Bruening, M. L. J Am Chem Soc 1999, 121 1978.
31. Fischer-Cripps, A. C. Nanoindentation; Springer-Verlag: New York, 2002.
32. Wang, T. C.; Cohen, R. E.; Rubner, M. F. Adv Mater 2002, 14, 1534.